

---

# Active Predictive Coding: A Unified Neural Framework for Learning Hierarchical World Models for Perception and Planning

---

**Rajesh P. N. Rao**

Paul G. Allen School of Computer Science and Engineering, University of Washington, Seattle

**Dimitrios C. Gklezacos**

**Vishwas Sathish**

{rao, gklezd, vsathish}@cs.washington.edu

## Abstract

Predictive coding has emerged as a prominent model of how the brain learns through predictions, anticipating the importance accorded to predictive learning in recent AI architectures such as transformers. Here we propose a new framework for predictive coding called active predictive coding which can learn hierarchical world models and solve two radically different open problems in AI: (1) how do we learn compositional representations, e.g., part-whole hierarchies, for equivariant vision? and (2) how do we solve large-scale planning problems, which are hard for traditional reinforcement learning, by composing complex action sequences from primitive policies? Our approach exploits hypernetworks, self-supervised learning and reinforcement learning to learn hierarchical world models that combine task-invariant state transition networks and task-dependent policy networks at multiple abstraction levels. We demonstrate the viability of our approach on a variety of vision datasets (MNIST, FashionMNIST, Omniglot) as well as on a scalable hierarchical planning problem. Our results represent, to our knowledge, the first demonstration of a unified solution to the part-whole learning problem posed by Hinton, the nested reference frames problem posed by Hawkins, and the integrated state-action hierarchy learning problem in reinforcement learning.

## 1 INTRODUCTION

Predictive coding (Rao and Ballard, 1999; Friston and Kiebel, 2009; Keller and Mrsic-Flogel, 2018; Jiang et al., 2021) has received growing attention in recent years as a model of how the brain learns models of the world through prediction and self-supervised learning. In predictive coding, feedback connections from a higher to a lower level of a cortical neural network (e.g., the visual cortex) con-

vey predictions of lower level responses and the prediction errors are conveyed via feedforward connections to correct the higher level estimates, completing a prediction-error-correction cycle. Such a model has provided explanations for a wide variety of neural and cognitive phenomena (Keller and Mrsic-Flogel, 2018; Jiang and Rao, 2022). The layered architecture of the cortex is remarkably similar across cortical areas (Mountcastle, 1978), hinting at a common computational principle, with superficial layers (layers 2-4) receiving and processing sensory information and deeper layers (layer 5) conveying outputs to motor centers (Sherman and Guillery, 2013). The traditional predictive coding model focused primarily on learning visual hierarchical representations and did not acknowledge the important role of actions in learning internal world models.

In this paper, we introduce Active Predictive Coding, a new model of predictive coding that combines state and action networks at different abstract levels to learn hierarchical internal models. The model provides a unified framework for solving three important AI problems as discussed below.

## 2 RELATED WORK

**Part-Whole Learning Problem.** Hinton and colleagues have posed the problem of how neural networks can learn to parse visual scenes into part-whole hierarchies by dynamically allocating nodes in a parse tree. They have explored networks that use a group of neurons to represent not only the presence of an object but also parameters such as position and orientation (Sabour et al., 2017; Kosiorek et al., 2019; Hinton et al., 2018; Hinton, 2021), seeking to overcome the inability of deep convolutional neural networks (CNNs) (Krizhevsky et al., 2012) which are unable to explain the images they classify in the way humans do, in terms of objects, parts and their locations. A major open question is how neural networks can learn to create parse trees on-the-fly using learned part-whole representations.

**Reference Frames Problem.** In a parallel line of research, Hawkins and colleagues (Hawkins, 2021; Lewis et al., 2019) have taken inspiration from the cortex and “grid cells” to propose that the brain uses object-centered

reference frames to represent objects, spatial environments and even abstract concepts. The question of how such reference frames can be learned and used in a nested manner for hierarchical recognition and reasoning has remained open.

### Integrated State-Action Hierarchy Learning Problem.

A considerable literature exists on hierarchical reinforcement learning (see (Hutsebaut-Buysse et al., 2022) for a recent survey), where the goal is to make traditional reinforcement learning (RL) algorithms more efficient through state and/or action abstraction. A particularly popular approach is to use options (Sutton et al., 1999), which are abstract actions which can be selected in particular states (in the option’s initiation set) and whose execution executes a sequence of primitive actions as prescribed by the option’s lower level policy. A major problem that has received recent attention (e.g., Bacon et al., 2016) is learning options from interactions with the environment. The broader problem of simultaneously learning state and action abstraction hierarchies has remained relatively less explored.

## 3 CONTRIBUTIONS OF THE PAPER

The proposed active predictive coding (APC) model addresses all three problems above in a unified manner using state/action embeddings and hypernetworks (Ha et al., 2017) to *dynamically generate and generalize* over state and action networks at multiple hierarchical levels. The APC model contributes to a number of lines of research which have not been connected before:

**Perception, Predictive Coding, and Reference Frame Learning:** APC extends predictive coding and related neuroscience models of brain function (Rao and Ballard, 1999; Friston and Kiebel, 2009; Jiang et al., 2021) to hierarchical sensory-motor inference and learning, and connects these to learning nested reference frames (Hawkins, 2021) for perception and cognition.

**Attention Networks:** APC extends previous hard attention approaches such as the Recurrent Attention Model (RAM) (Mnih et al., 2014) and Attend-Infer-Repeat (AIR) (Eslami et al., 2016) by learning structured hierarchical strategies for sampling the visual scene.

**Hierarchical Planning and Reinforcement Learning:** APC contributes to hierarchical planning/reinforcement learning research (Hutsebaut-Buysse et al., 2022; Botvinick et al., 2009) by proposing a new way of simultaneously learning abstract macro-actions or options (Sutton et al., 1999) and abstract states.

**General Applicability in AI:** When applied to vision, the APC model learns to hierarchically represent and parse images into parts and locations. When applied to RL problems, the model can exploit hypernets to (a) define a state hierarchy, *not merely through state aggregation*, but by *abstracting transition dynamics at multiple levels*, and (b) potentially generalize learned hierarchical states and actions (options) to novel scenarios via interpolation/extrapolation

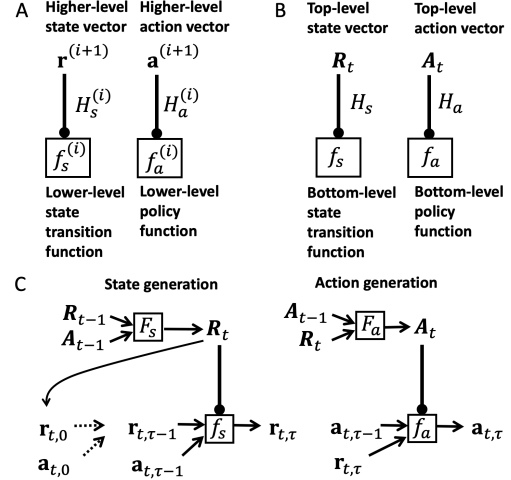


Figure 1: **Active Predictive Coding Generative Module:** (A) Canonical generative module for the APC model. The lower level functions are generated via hypernetworks based on the current higher level state and action embedding vectors. All functions (in boxes) are implemented as recurrent neural networks (RNNs). Arrows with circular terminations denote generation of function parameters (here, neural network weights and biases). (B) Two-level model used in this paper. (C) Generation of states and actions in the 2-level model based on past states and actions.

in the input embedding space of the hypernetworks.

Our approach brings us closer towards a neural solution to an important challenge in both AI and cognitive science (Lake et al., 2017): how can neural networks learn hierarchical compositional representations that allow new concepts to be created, recognized and learned?

## 4 ACTIVE PREDICTIVE CODING MODEL

The APC model implements a hierarchical version of the traditional Partially Observable Markov Decision Process (POMDP) (Kaelbling et al., 1998; Rao, 2010), with each level employing a state network and an action network.

Figure 1A shows the canonical generative module for the APC model. The module consists of (1) a *higher level state embedding vector*  $\mathbf{r}^{(i+1)}$  at level  $i + 1$ , which uses a function  $H_s^i$  (implemented as a *hypernetwork* (Ha et al., 2017))<sup>1</sup> to generate a lower level state transition function  $f_s^i$  (implemented as an RNN), and (2) a *higher level action embedding vector*  $\mathbf{a}^{(i+1)}$ , which uses a function (hypernetwork)  $H_a^i$  to generate a lower level *option/policy function*  $f_a^i$  (implemented as an RNN). The state and action networks at the lower level are generated independently (by the higher level state/action embedding vectors) but exchange information

<sup>1</sup>See Supplementary Materials for an alternate neural implementation of the APC model using higher-level embedding-based inputs to lower-level RNNs.

horizontally within each level as shown in Figure 1C: the state network generates the next state prediction based on the current state and action while the action network generates the current action based on the current state and previous action. In our current implementation, the lower level RNNs execute for a fixed number of time steps before returning control back to the higher level.<sup>2</sup> For the present paper, we focus on a two-level model (with a top level and bottom level) as shown in Figures 1B-C.

#### 4.1 Inference in the Active Predictive Coding Model

Inference involves estimating the state and action vectors at multiple levels based on the sequence of inputs produced by interacting with the environment in the context of a particular task or goal. The top level runs for  $T_2$  steps (referred to as “macro-steps”). For each macro-step, the bottom level runs for  $T_1$  “micro-steps”. As shown in Figure 1C,  $F_s, F_a$  are the top level state and action networks respectively, and  $R_t, A_t$  are the recurrent activity vectors of these networks (i.e., the top level state and action embedding vectors) at macro-step  $t$ . We use the notation  $f(\cdot; \theta)$  to denote a network parameterized by  $\theta = \{W_l, b_l\}_{l=1}^L$ , the weight matrices and biases for all the layers. The bottom level state and action RNNs are denoted by  $f_s(\cdot; \theta_s)$  and  $f_a(\cdot; \theta_a)$ , while their activity vectors are denoted by  $r_{t,\tau}$  and  $a_{t,\tau}$  respectively ( $t$  ranges over macro-steps,  $\tau$  over micro-steps).

##### 4.1.1 Higher-Level Inference and Reference Frame Generation

At each macro-step  $t$ , the top level state RNN  $F_s$  produces a new state embedding vector  $R_t$  based on the previous state and action embedding vectors. This higher level state  $R_t$  defines a new “reference frame” for the lower level to operate over as follows:  $R_t$  is fed as input to the state hypernetwork  $H_s$  to generate the lower level parameters  $\theta_s(t) = H_s(R_t)$  specifying a dynamically generated bottom-level state RNN characterizing the state transition dynamics locally (e.g., local parts and their transformations in vision (see Section 5), navigation dynamics in a local region of a building (see Section 6)). Figure 2 (a) illustrates this top-down generation process.

The current state  $R_t$  is also input to the action/policy RNN  $F_a$  which outputs an action embedding vector  $A_t$  (a macro-action/option/sub-goal) appropriate for the current task/goal given current state  $R_t$  (Figure 2 (a)). This embedding vector  $A_t$  is used as input to a non-linear function, implemented by the hypernetwork  $H_a$ , to dynamically generate the parameters  $\theta_a(t) = H_a(A_t)$  of the lower-level action RNN, which implements a policy to generate primitive actions suitable for achieving the sub-goal associated with  $A_t$ . Since reinforcement learning or planning require exploration, the output of an action network at any level can

<sup>2</sup>Future implementations will explore the use of termination functions (Sutton et al., 1999; Eslami et al., 2016) to allow a variable number of time steps at each level and for each input.

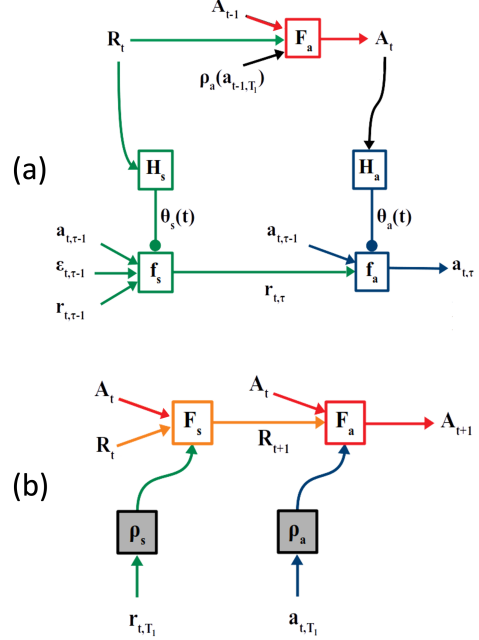


Figure 2: **Inference in the Active Predictive Coding Model:** (a) Dynamic generation of bottom-level state RNN  $f_s$  and action RNN  $f_a$  (“sub-programs”) from top-level state vector  $R_t$  and action vector  $A_t$ . This diagram elaborates the one in Figure 1C. (b) Update of top-level state  $R_t$  and action  $A_t$  based on feedback (via networks  $\rho_s$  and  $\rho_a$ ) upon bottom-level sub-program termination.

be regarded as the mean value of a Gaussian with fixed variance (Mnih et al., 2014) or as a categorical representation (Hafner et al., 2021) to sample an action.

##### 4.1.2 Lower-Level Inference and Interaction with the Higher Level

At the beginning of each micro-step, the higher-level state  $R_t$  is used to initialize the bottom-level state vector via a small feedforward network  $\text{Init}_s$  to produce  $r_{t,0} = \text{Init}_s(R_t)$ . Each micro-step proceeds in a manner similar to a macro-step. The bottom-level action RNN, which was generated by higher-level state  $R_t$ , produces the current action  $a_{t,\tau}$  based on the current lower level state and previous action (Figure 2 (a) lower right). This action (e.g., eye movement or body movement) results in a new input being generated by the environment for the bottom (and possibly higher) state network.

To predict this new input, the lower-level state vector  $r_{t,\tau}$  is fed to a generic decoder network  $D$  to generate the prediction  $\hat{I}_{t,\tau}$ . This predicted input is compared to the actual input to generate a prediction error  $\epsilon_{t,\tau} = I_{t,\tau} - \hat{I}_{t,\tau}$ . Following the predictive coding model (Rao and Ballard, 1999), the prediction error is used to update the state vector via the state network:  $r_{t,\tau+1} = f_s(r_{t,\tau}, \epsilon_{t,\tau}, a_{t,\tau}; \theta_s(t))$  (Figure 2 (a) lower left).

At the end of each macro-step (after  $T_1$  bottom-level micro-steps have finished executing), the top level state RNN activity vector is updated using the final bottom-level state vector:  $R_{t+1} = F_s(R_t, A_t, \rho_s(r_{t,T_1}))$  where  $\rho_s()$  is a single-layer state “feedback” network (see Figure 2 (b) left side). The top-level action RNN then produces the action vector  $A_{t+1}$  based on state  $R_{t+1}$  and lower level feedback  $\rho_a(a_{t,T_1})$  (Figure 2 (b) right side), and the process continues. The above steps correspond to a sub-program in the state/action hierarchy terminating and returning its result to be integrated by its parent. Note that more levels can be added by having  $F_s, F_a$  be dynamically generated by another parent level, and so on.

#### 4.2 Training the Active Predictive Coding Model

Since the state networks are task-agnostic and geared towards capturing the dynamics of the world, they are trained using self-supervised learning by minimizing prediction errors (here, via backpropagation). The action networks are trained to minimize total expected task loss: this can be done using either reinforcement learning or planning with the help of the state networks. In Section 5 (learning equivariant vision), we illustrate the use of the REINFORCE algorithm (Williams, 1992) for training the action networks while in Section 6 (learning navigation), we illustrate the use of planning but note that the APC framework is flexible and allows either approach for estimating actions.

### 5 APPLICATION TO EQUIVARIANT VISION AND PART-WHOLE LEARNING

A long standing problem in computer vision and cognitive science is: how can neural networks learn intrinsic references frames for objects and parse visual scenes into part-whole hierarchies by dynamically allocating nodes in a parse tree (Hinton, 2021)? Human vision provides an important clue. Unlike CNNs which process an entire scene, human vision is an active sensory-motor process, sampling the scene via eye movements to move the high-resolution fovea to appropriate locations and accumulating evidence for or against competing visual hypotheses (Wedel et al., 2022). As described below, the APC model is well-suited to emulating the sensory-motor nature of human vision, given its integrated state and action networks.

#### 5.1 APC Solution to the Equivariant Vision and Part-Whole Learning Problem

For equivariant vision and part-whole learning, the actions in the APC model emulate eye movements (or “attention”) and correspond to moving a “glimpse sensor” (Mnih et al., 2014) which extracts high-resolution information about a small part of a larger input image. Given an input image  $I$  (of size  $N \times N$  pixels), this sensor,  $G$ , takes in a location  $l$  and a fixed scale fraction  $m$ , and extracts a square

glimpse/patch  $g = G(I, l, m)$  centered at  $l$  and of size  $(mN) \times (mN)$ . The location  $l$  to fixate next is selected by the bottom level action network within the reference frame specified by the higher level, while the bottom state network generates a prediction of the glimpse, the prediction error being used for updating the state and for learning.

In more detail, at each macro-step  $t$ , the top level action vector  $A_t$  generates two values: (a) a location  $L_t$  and (b) a macro-action (or option)  $z_t$ . The location  $L_t$  is used to restrict the bottom level to a sub-region  $I_t^{(1)} = G(I, L_t, M)$  of scale  $M$  centered around  $L_t$ , corresponding to a new frame of reference selected by the top level within the input image. The option  $z_t$ , which operates over this frame of reference, is used as an embedding vector input to the hypernetwork  $H_a$  to generate the parameters of the bottom level action RNN. For exploration during reinforcement learning, we treat the output of the location network as a mean value  $\bar{L}_t$  and add Gaussian noise with fixed variance to sample an actual location:  $L_t = \bar{L}_t + \epsilon$ , where  $\epsilon \sim \mathcal{N}(0, \sigma^2)$ . We do the same for the option  $z_t$ .

Based on the current bottom-level state and action, the bottom-level action RNN generates a new action  $a_{t,\tau}$ . A location  $l_{t,\tau}$  is chosen as a function of  $a_{t,\tau}$ , resulting in a new glimpse image  $g_{t,\tau} = G(I_t^{(1)}, l_{t,\tau}, m)$  of scale  $m$  centered around  $l_{t,\tau}$  and yielding a nested reference frame within the larger reference frame of  $I_t^{(1)}$  specified by the higher level. The bottom level follows the same Gaussian noise-based exploration strategy for sampling locations as the top level. The bottom-level state vector  $r_{t,\tau}$ , along with locations  $L_t$  and  $l_{t,\tau}$ , are fed to a generic decoder network  $D$  to generate the predicted glimpse  $\hat{g}_{t,\tau}$ . Following the predictive coding model (Rao and Ballard, 1999), the resulting prediction error  $\epsilon_{t,\tau} = g_{t,\tau} - \hat{g}_{t,\tau}$  is used to update the state vector:  $r_{t,\tau+1} = f_s(r_{t,\tau}, \epsilon_{t,\tau}, l_{t,\tau}; \theta_{(s)}(t))$ . For the results below, the state networks at both levels were trained to minimize image prediction errors while the action networks were trained using reinforcement learning (the REINFORCE algorithm (Williams, 1992)).

#### 5.2 Results

We first tested the APC model on the task of sequential part/location prediction and image reconstruction of objects in the following datasets: (a) MNIST: Original MNIST dataset of 10 classes of handwritten digits. (b) Fashion-MNIST: Instead of digits, the dataset consists of 10 classes of clothing items. (c) Omniglot: 1623 handwritten characters from 50 alphabets, with 20 samples per character. For our APC models, we used 3 macro- and 3 micro-steps (except 4 macro-steps for Omniglot). A single dense layer, together with an initial random glimpse was used to initialize the state and action vectors of the top level (see Supplementary Materials for details).

**Learning to Parse Images into Parts and Perceptual Stability.** Figure 3 shows an example of a learned parsing

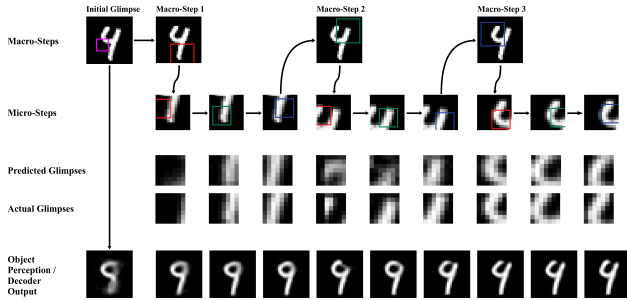


Figure 3: **Learned Two-Level Parsing Strategy and an Illustration of Perceptual Stability in the presence of Eye Movements:** 1st row: Initialization glimpse (purple box) and sampled top-level reference frames (red, green, blue boxes), 2nd row: Sampled bottom level parts within each top-level frame, 3rd & 4th rows: Predicted versus actual parts/glimpses, and 5th row: “Perception” of the model (object reconstructed from current network state) over time. Note the perceptual stability in the model despite jumps in the sampled glimpses (see row of Actual Glimpses) as the object hypothesis is gradually refined based on accumulated evidence.

strategy by a two-level APC model for an MNIST digit. The top-level learned to cover the input image sufficiently while the bottom level learned to parse sub-parts inside the reference frame computed by the higher level.

Figure 3 also provides an explanation for why human perception can appear stable despite dramatic changes in our retinal images as our eyes move to sample a scene: the last row of the figure shows how the model maintains a visual hypothesis that is gradually refined and which does not exhibit the kind of rapid changes seen in the sampled images (“Actual Glimpses” in Figure 3).

Figure 4 shows a learned part-whole hierarchy for an MNIST input, in the form of a parse tree of parts and sub-parts (strokes and mini-strokes) with their locations. The model learns different parsing strategies and different part-whole hierarchies for different classes of objects, as seen in Figure 5 for two different clothing items from the Fashion-MNIST dataset (T-shirt versus sneaker). Top-level part locations across all classes are shown in Figure 6.

**Prediction of Parts and Pattern Completion.** To investigate the predictive and generative ability of the model, we had the model “hallucinate” different parts of an object by setting the prediction error input to the lower level network to zero. This disconnects the model from the input, forcing it to predict the next sequence of parts and “complete” the object. Figure 7a shows that the model has learned to generate plausible predictions of parts given an initial glimpse.

**Transfer Learning.** We tested transfer learning for reconstruction of unseen character classes for the Omniglot dataset. We trained a two-level APC model to reconstruct

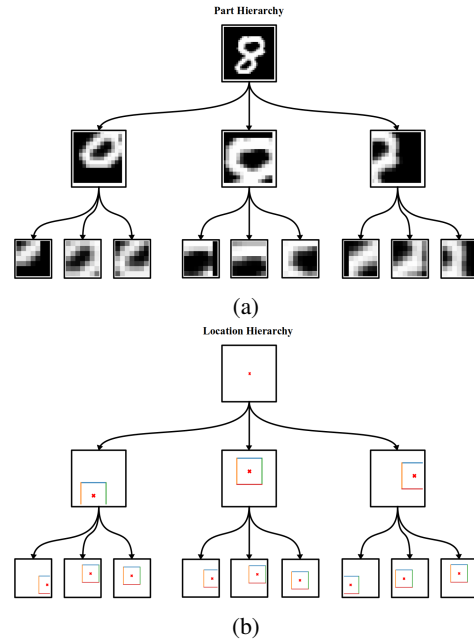


Figure 4: **Example Parse Tree with Inferred Locations of Parts:** Hierarchy of (a) sampled parts and (b) sampled locations, inducing a hierarchy of reference frames.

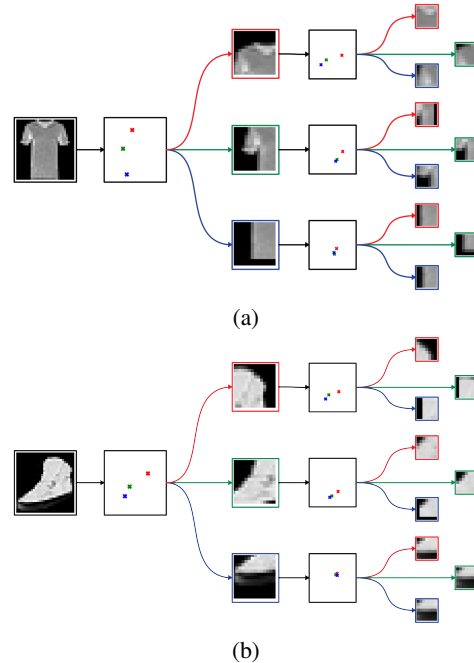


Figure 5: **Class-Based Hierarchical Representation of Object Parts and Locations:** Average sampled locations per class, together with sampled parts for one specific example for (a) the T-shirt and (b) the sneaker classes. The order of sampled locations within each frame of reference is 1st: red, 2nd: green and 3rd: blue.

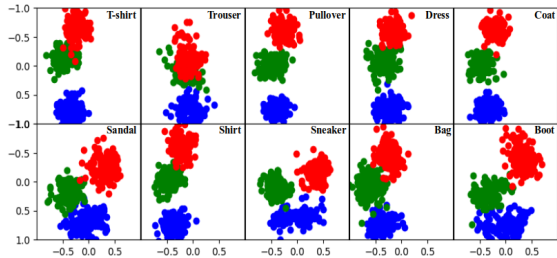


Figure 6: **Top-level Part Locations for Fashion-MNIST Examples by Class:** Red: first, Green: second and Blue: third location. Note the differences in top-level action strategies between vertically symmetric items (shirts, trousers, bags) and footwear (sandals, sneakers, boots).

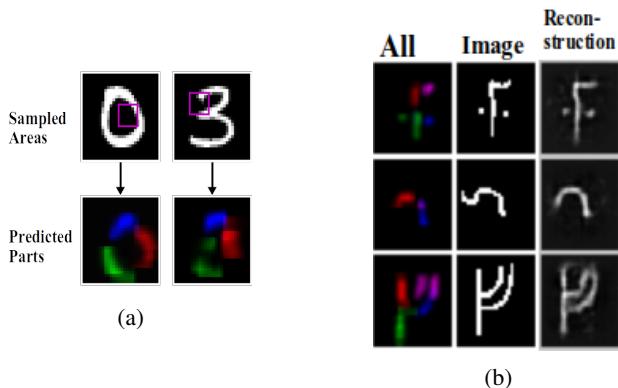


Figure 7: **Prediction of Parts, Pattern Completion and Transfer Learning:** (a) Given only an initialization glimpse (purple box) for an input image (here, a 0 and a 3 from MNIST), an APC model trained on MNIST predicts its best guess of the parts of the object and their locations (colored segments in row below). (b) APC model trained on Omniglot can transfer its learned knowledge to predict parts of previously unseen character classes. First column: all the predicted parts. Middle column: input from a novel class. Last column: APC model reconstruction.

examples from 85% of classes from each Omniglot alphabets. The rest of the classes were used to test transfer: the trained model had to generate new programs (via the state and action hypernets) to predict parts for new character classes for each alphabet. The model successfully performed this transfer task (Table 1 and Figure 7b).

**Ablation Studies.** To test the utility of having two levels of abstraction, we compared the image reconstruction performance of the two-level APC model (APC-2) to a one-level model (APC-1). To test the importance of intelligent sampling of the image, we used a Randomized Baseline model RB, which samples glimpses (same size glimpses as APC-1 and APC-2) from  $T$  i.i.d. locations ( $T$  same as for APC-1 and APC-2, i.e., 9 for MNIST/FMNIST, 12 for Omniglot), extracts an average feature vector and feeds this to a feed-

	MNIST	FMNIST	Om-Tst	Om-Trn
RB	0.0120	0.0145	0.0307	0.0301
APC-1	0.0114	<b>0.0138</b>	0.0324	0.0323
APC-2	<b>0.0085</b>	<b>0.0138</b>	<b>0.0227</b>	<b>0.0226</b>

Table 1: **Ablation Studies: Reconstruction Mean-Squared-Error (per pixel) for Different Models Across Datasets:** See text for details. FMNIST, Om-Tst and Om-Trn denote Fashion-MNIST, the Omniglot test and transfer datasets respectively.

forward network to reconstruct the image. As shown in Table 1, APC-2 outperforms or matches APC-1 and RB. APC-2 also outperforms RB and APC-1 on the Omniglot transfer learning task (“Om-Trn” column in Table 1). We also considered classification as the APC task but found reconstruction to be more suited to part-whole learning (see Supplementary Materials).

## 6 APPLICATION TO HIERARCHICAL PLANNING

We now show that the same APC framework used for learning part-whole hierarchies can also be used for learning hierarchical world models for efficient planning. We introduce a new compositional, scalable “multi-rooms” building navigation task to illustrate this. The APC model’s state-action hierarchy lends itself naturally to other RL problems as well, which we hope to demonstrate in future work.

### 6.1 APC Solution to Hierarchical Planning

Consider the problem of navigating from any starting location to any goal location in a large “multi-rooms” building environment such as the one in Figure 8 (a) (gray: walls, blue circle: agent, green square: current goal). In the traditional non-hierarchical RL approach, the states are the discrete locations in the grid, and actions are going north (N), east (E), south (S) or west (W). A large reward (+10) is received at the goal location, with a small negative reward (-0.1) for each action to encourage shortest paths.

**Problems with traditional RL.** There are three major problems with the traditional RL approach: (1) Sample inefficiency: As the environment gets larger, the number of interactions with the environment required to learn the value function explodes, (2) Risk of catastrophic consequences: Taking actual actions in the real-world to estimate the value function might have catastrophic consequences (injury or death), and (3) Inflexibility: Even after learning the value function to reach a particular goal, any change in the goal requires learning a whole new value function.

**How the APC model solves these problems.** First, note that just as an object (e.g., an MNIST digit in Section 5) consists of the same parts (e.g., strokes) occurring at different locations, the multi-rooms environment in Figure 8 is

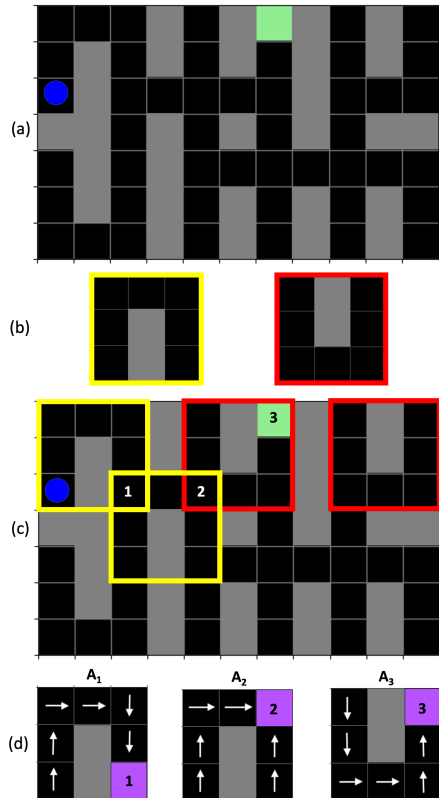


Figure 8: **The Multi-Rooms Building Navigation Problem and State-Action Hierarchy.** The problem of navigating in a large building (blue: agent location, gray: walls, green: goal) can be reduced to planning using high-level states ((b) and (c)) and actions (d). See text for details.

also made up of the same two components (“Room types” R1 and R2), shown in Figure 8 (b), occurring at different locations (some example locations highlighted by yellow and red boxes in Figure 8 (c)). These components form part of the higher-level states in the APC and are defined by state embedding vectors R1 and R2, which can be trained to generate, via the hypernet  $H_s$  (Figure 2), the lower-level transition functions  $f_s$  for rooms R1 and R2 respectively.

Next, similar to how the APC model was able to reconstruct an image in Section 5 using higher-level action embedding vectors to generate policies and actions (locations) to compose parts using strokes, the APC model can compute higher-level action embedding vectors  $A_i$  (option vectors) for the multi-rooms world that generate, via hypernet  $H_a$  (Figure 2), lower-level policies  $f_a$  which produce primitive actions (N, E, S, W) to reach a goal  $i$  encoded by  $A_i$ .

**Local reference frames allow policy re-use and transfer.** Figure 8 (d) illustrates the bottom-level policies for three such action embedding vectors  $A_1$ ,  $A_2$  and  $A_3$ , which generate policies for reaching goal locations 1, 2, and 3 respectively. Note that the  $A_i$  are defined with respect to higher-level state R1 or R2. Defining these policies to oper-

ate within the local reference frame of the higher-level state R1 or R2 (regardless of global location in the building) confers the APC model with enormous flexibility because the *same policy can be re-used at multiple locations* to solve local tasks (here, reach sub-goals within R1 or R2). For example, to solve the navigation problem in Figure 8 (c), the APC model only needs to plan and execute 3 higher-level actions or options:  $A_1$  followed by  $A_2$  followed by  $A_3$ , compared to planning a sequence of 12 lower-level actions to reach the same goal. Finally, since the  $A_i$  embedding space of options is continuous, there is an unprecedented opportunity for the APC model to exploit properties of this space (such as smoothness) to interpolate or extrapolate to create and explore new options for transfer learning; this possibility will be explored in future work.

## 6.2 Results

We used a simple curriculum to train the two-level APC model as follows.

**States.** For simplicity, we assume the higher-level states capture  $3 \times 3$  local reference frames and are defined by an embedding vector generating the transition function for “room type” R1 or R2, along with the location for this local reference frame in the global frame of the building.

**Actions.** The lower-level action network is trained to map a higher-level action embedding vector  $A_i$  to a lower-level policy that navigates the agent to a particular goal location  $i$  within R1 or R2. For the current example, eight embedding vectors  $A_1, \dots, A_8$  were trained, using REINFORCE-based RL (Williams, 1992), to generate via the hypernet  $H_a$  eight lower-level policies to navigate to each of the four corners of room types R1 and R2.

**Prediction and Planning.** The higher-level state network  $F_s$  was trained to predict the next higher-level state (decoded as an image of room type R1 or R2, plus its location) given the current higher-level state and higher-level action. The trained higher-level state network  $F_s$  was used for planning at each step a sequence of 4 higher-level actions using random-sampling shooting model-predictive control (MPC) (Richards, 2004): random state-action trajectories of length 4 were generated using  $F_s$  by starting from the current state and picking one of the four random actions  $A_i$  for each next state; the action sequence with the highest total reward was selected and its first action was executed. Figure 9 shows an example of this high-level planning and MPC process using the trained APC model.

**Performance Comparison with Traditional RL and Planning on Goal-Changing Navigation Task.** We compared the two-level APC model with both a heuristic lower-level-only planning algorithm and a REINFORCE-based RL algorithm using primitive states and actions. The task involved navigating to a randomly selected goal location in a building environment (as in Figure 8 (a)), with the goal location changing after some number of episodes. Figure 10 (a) shows how the APC model, after an initial period spent on learning the hypernet  $H_a$  to generate the lower-level op-

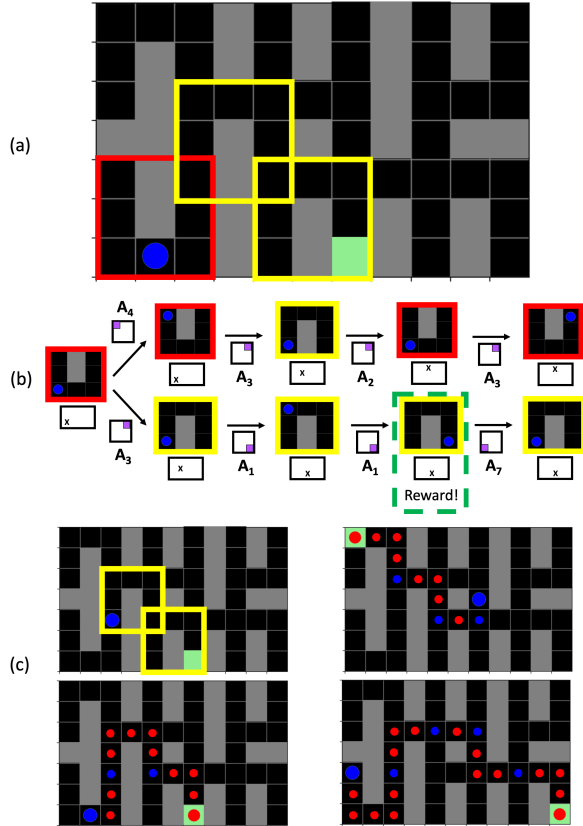


Figure 9: **Planning and Model Predictive Control.** To navigate to the green goal in (a), the agent (blue) uses its learned high-level state network to sample  $N$  high-level state-action trajectories ( $N = 2$  in (b)), picks the sequence with highest total reward, executes this sequence’s first action to reach the location in (c) (top left), and repeats to reach the goal with 3 high-level actions (bottom left in (c)). Two more planning examples are shown on the right in (c) (small red dot: intermediate location; small blue dot: intermediate goal). In (b), high-level state is depicted by predicted R1 or R2 image and its location  $X$  in global frame, action by its goal (purple) in a square local frame.

tions, is able to cope with goal changes and successfully navigate to each new goal by sequencing high-level actions (+10 reward for goal; -0.1 per primitive action). The RL algorithm, on the other hand, experiences a drop in performance after a goal change and does not recover even after 500 episodes. Figure 10 (b) demonstrates the efficacy of APC’s higher-level planning compared to lower-level planning (MPC using random sequences of 4 primitive future actions; Euclidean distance heuristic; see Supplementary Materials for details): the average number of planning steps to reach the goal increases dramatically for larger distances from the goal for the lower-level planner compared to higher-level planning by the APC model.

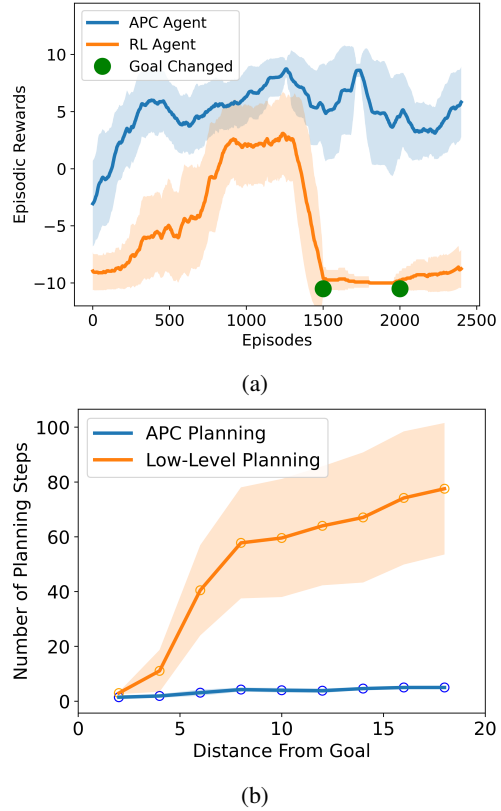


Figure 10: **APC Model Performance.** See text for details.

## 7 CONCLUSION

We have presented, to our knowledge, the first demonstration of a unified solution to the part-whole learning problem (Hinton, 2021), the nested reference frames problem (Hawkins, 2021), and the integrated state-action hierarchy learning problem in reinforcement learning (Hutsebaut-Buysse et al., 2022). Our APC model is inspired by the growing evidence for predictive sensory-motor processing in the cortex (Schneider et al., 2018; Keller and Mrsic-Flogel, 2018). The APC model for equivariant vision employs “eye movements” for visual sampling, and performs end-to-end learning and parsing of part-whole hierarchies from images. We also showed how the same APC framework provides a flexible approach to hierarchical planning and action selection. Given the growing interest in predictive coding as a model for the cortex, our results showing two very different applications of the same APC model lend further support to the hypothesis of a possible common computational principle operating across cortex (Mountcastle, 1978). Current limitations of the model include the fixed number of time steps used at each level and using only a two-level hierarchy. Future work will explore deeper versions of the model, comparisons to neuroscience data, and more sophisticated planning/RL methods to enable the model to scale to more complex tasks.



---

## Supplementary Materials

# Active Predictive Coding: A Unified Neural Framework for Learning Hierarchical World Models for Perception and Planning

---

## 1 Active Predictive Coding for Equivariant Vision

### 1.1 Experimental Details

#### 1.1.1 Parameter Settings

For the active predictive coding (APC) model for vision introduced in Section 5, for all datasets (MNIST, FMNIST, Omniglot and affNIST<sup>1</sup>), the top-level action and state RNN activity vectors were of size 256, while the lower level ones were of size 32 for MNIST, Fashion-MNIST and 64 for Omniglot. Both hypernetworks  $H_s$  and  $H_a$  consisted of four layers with sizes 256, 256, 64 and  $|\theta_s|$  or  $|\theta_a|$ . The last two layers had linear activation functions. Since the number of units of the last layer was equal to the number of parameters of  $f_a$  or  $f_s$ , the middle layer functions as a bottleneck layer.  $F_a$  and  $F_s$  were implemented as RNNs with structure similar to the network used in RAM (Mnih et al., 2014). The option vectors  $\mathbf{z}$  were of size 32. RELU activations were employed throughout the model apart from the last level of the reconstruction network (to avoid “dead” pixels). The glimpse scales were set such that  $I^{(1)}$  was  $14 \times 14$  and  $g_{t,\tau}$   $7 \times 7$  pixels. The sizes of MNIST and Fashion-MNIST images are  $28 \times 28$  pixels, whereas we downsampled Omniglot characters to  $32 \times 32$  pixels.

For Omniglot, we reserved 85% (rounded down) of the character classes in each alphabet as part of our training set. The rest of the character classes were used as the transfer set. Within the training classes, we reserved 3 examples from each character class for the validation set and another 3 for the test set.

#### 1.1.2 Initialization

We utilize random glimpses to initialize the top-level state and action vectors. A random glimpse is generated at location  $l_{\text{init}} \sim \mathcal{U}[-0.5, 0.5]$ . This initialization glimpse  $g_{\text{init}}$ , together with a small trainable initialization network, initializes the state vector  $\mathbf{R}_0$ . The action vector is initialized using  $F_a$  and  $\mathbf{R}_0$  by setting the previous action vector and feedback  $\rho_A$  to all-zeroes vectors.

#### 1.1.3 Training Settings

For training, we used the Adam optimizer (Kingma and Ba, 2015). For all datasets, we trained the model for a number of epochs with a learning rate of 0.0001 (first phase). Then we reduced the learning rate to 0.00001 (second phase). The number of epochs for each phase and dataset are shown in Table 1.

	First phase	Second phase
<b>MNIST</b>	1000	200
<b>FMNIST</b>	1000	200
<b>Omniglot</b>	10000	2000
<b>affNIST</b>	2000	500

Table 1: Training schedules for each dataset.

---

<sup>1</sup>affNIST is only used for the comparison in Supplementary Materials Section 1.3.

### 1.1.4 Location Penalty

Ideally the APC model for vision in Section 5 would avoid generating locations exceeding the boundaries of the image. Several implementations of RAM (Mnih et al., 2014) use clipping or the hyperbolic tangent activation function. In practice, we found that constraining the locations via an appropriate penalty was more effective. We calculate a threshold  $c$  so that if a glimpse is centered  $c$  units away from the image boundary ( $l \in [-1.0 + c, 1.0 - c]$ ), then the glimpse resides entirely within that boundary. We then apply a thresholded version of  $\ell_2$  normalization:

$$L_{\text{reg}}(l) = (\text{LRelu}(l - c))^2 + (\text{LRelu}(-l - c))^2 - 2(\alpha c)^2$$

where LRelu is the leaky rectified linear unit with  $\alpha = 0.2$ . The structure of this penalty can be seen in Figure 1.

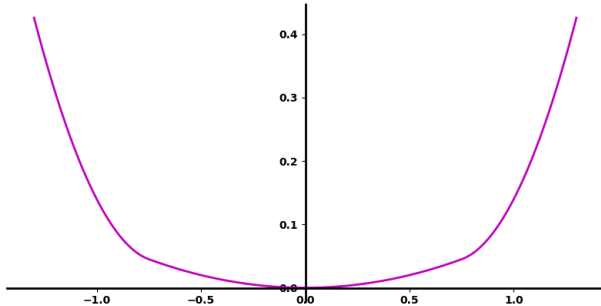


Figure 1: APC location penalty function for  $c = 0.75$ .

## 1.2 Using Classification instead of Reconstruction as the APC Task

We initially considered classification as a task for the APC model. A previous model (Mnih et al., 2014) showed that using a single glimpse randomly sampled from the entire input image achieves 57.15% classification accuracy on the MNIST dataset. We found that our RB baseline with three random glimpses already achieved 93.1% classification accuracy. This suggested to us that rather than classification (where random glimpses appear to give good accuracies at least for the MNIST dataset), the task of reconstructing an object, such as an MNIST digit, might be a more appropriate task for learning and enumerating the parts of an object. We therefore chose image reconstruction as the task for testing the APC model.

## 1.3 Hypernetworks versus Traditional Embedding-Based Alternate Model

	affNIST
APC-2-Embedding	0.0110
APC-2-Hypernet	0.0105

Table 2: Hypernetworks vs. Embedding-Based Alternative for Generating Sub-Programs for affNIST.

An alternative to using hypernetworks to generate the state and action sub-programs is to use an embedding-based approach (Galanti and Wolf, 2020): the higher-level embedding vector is fed as input to a feedforward network and its output is concatenated with the input to the bottom level RNN. We compared the two approaches on the reconstruction task for affNIST, a dataset that consists of MNIST digits embedded in a  $40 \times 40$ -pixel frame and transformed via random affine transformations. The results, shown in Table 2, indicate that hypernetworks provide a more efficient abstraction for sub-program generation. See (Galanti and Wolf, 2020) for a theoretical discussion of the advantages of hypernetworks over the embedding approach.

## 2 Active Predictive Coding for Hierarchical Planning

### 2.1 APC Model Components

To test hierarchical planning, we introduce a new task involving navigation in a compositional environment (as shown in Figure 8 of the paper). The complete APC model for this task can be decoupled into independent trainable components corresponding to each level of a hierarchy. For training data, we collect the state-action tuples  $(\mathbf{r}_\tau, \mathbf{a}_\tau, \mathbf{r}_{\tau+1})$  and

$(\mathbf{R}_t, \mathbf{A}_t, \mathbf{R}_{t+1})$  for each episode (see Figure 2 from the paper for details) and use it to train lower-level networks ( $f_s, f_a$ ) and higher-level networks ( $F_s, F_a$ ) respectively.

### 2.1.1 Lower-Level Networks

The lower networks ( $f_s, f_a$ ) are generated by hypernetworks  $H_s$  and  $H_a$  in Figure 2 in the paper. In the comparison with the APC hierarchical planner (see below),  $f_s$  was chosen to be the ground truth environment transition model to give the lower-level planner the best possible advantage when comparing to the APC planner. The parameters  $\theta_a$  of action policy network  $f_a$  was generated from the hypernetwork  $H_a$  that takes the abstract action vector  $\mathbf{A}_i$  as input.  $H_a$  is initialized with principled weight initialization strategies that have proven benefits for hypernetworks (Chang et al., 2020). Our hypernetwork is a simple 4-layer dense neural net with ReLU activations.  $H_a$  outputs parameters for a 3-layer policy network  $f_a$ . This policy network allows sampling of actions in an on-policy fashion, and generates the tuples  $(\mathbf{r}_t, \mathbf{a}_t, G_t, \mathbf{r}_{t+1})$  where  $G_t$  is the discounted reward. The entire model is trained using the episodic REINFORCE algorithm (Sutton et al., 2000; Williams, 1992). Baseline methods are used to reduce variance in the gradient computation. We also apply an  $L_2$  regularization constraint on the output action logits, which has been shown to be highly beneficial in improving the stability of training. Formally,

$$\theta_{a,i} = H_a(\mathbf{A}_i); \quad \mathbf{a}_t \sim f_a(\mathbf{r}_t; \theta_{a,i})$$

$$L_{REINFORCE} = J(\theta_{H_a}, \theta_{a,i}) = \sum_{t=1}^{T_1} \left[ \underbrace{-\log \pi(\mathbf{a}_t | \mathbf{r}_t; f_a)(G_t - b(\mathbf{r}_t))}_{\text{Policy Gradient Loss}} + \underbrace{\|f_a(\mathbf{r}_t; \theta_{a,i})\|_2^2}_{L_2 \text{ Loss}} \right]$$

Here  $T_1$  is the length of the episode and  $b(\mathbf{r}_t)$  is the baseline value for the state  $\mathbf{r}_t$ . We note that the APC architecture is independent of the RL algorithm used to train the model. More efficient Actor-Critic and DDPG methods will be explored in our future work.

### 2.1.2 Higher-Level Networks

To illustrate the performance of the APC model on navigation tasks, we choose eight higher-level actions ( $\mathbf{A}_1, \mathbf{A}_2, \dots, \mathbf{A}_8$ ), one for each subgoal within the two room types  $R_1$  and  $R_2$ . Each vector  $\mathbf{A}_i$  is a one-hot vector representing this subgoal. To perform hierarchical planning, we learn the higher-level state transition network  $F_s$  which predicts the next higher-level state  $\mathbf{R}_{t+1}$  given the current higher-level state  $\mathbf{R}_t$  and action  $\mathbf{A}_t$ . The network  $F_s$  receives as input the concatenated representation containing room location and an image of the room, and predicts the same representation for the next higher-level time step. We implement the recurrent network  $F_s$  as a simple 4 layer neural network with one recurrent LSTM layer, with ReLU and eLU activations. The reconstruction error (mean square error) between predicted and actual inputs was used as the loss function to train  $F_s$  via gradient descent and backpropagation.

The higher action policy  $F_a$  which outputs  $\mathbf{A}_t$  given  $\mathbf{R}_t$  and  $\mathbf{A}_{t-1}$  can be trained with the planned action sequences that were successful in navigating to the goal. This will be explored in future work.

## 2.2 Experimental Details

Table 3 lists the important hyperparameters used to train our APC model for planning. The code snippet to train the hypernetwork agent is provided in Listing 1. The goal of our planning experiments was to show that (1) APC model can be extended to navigation and RL domains, (2) APC is robust to changes in goals and (3) the hierarchy can be exploited to plan at exponentially faster rates. Here, we discuss the experimental setup we used to help achieve these goals.

### 2.2.1 Comparison with Traditional RL Agent

To illustrate the APC model’s zero-shot planning ability in a goal-changing navigation task, we compared the APC model to a traditional RL agent with no hierarchy. The RL agent is a relatively large recurrent LSTM neural net with layers [128, 256, 128, 32, 4]. This neural net acts as a policy and takes current primitive states (locations)  $s_t$  as input. Primitive actions are sampled from the action probabilities output by this network. This agent is trained via REINFORCE (with baseline), similar to the lower level policy networks in the APC model, in an online and episodic fashion.

During training, the goal was changed when the RL agent had learned a reasonable policy (see Figure 10 (a) in the paper). Unsurprisingly, the episodic rewards drop rapidly with the change in goals. This is not the case for our APC agent, which

Hyperparameters	Selected Value
Agent Learning Rate ( $\alpha_a$ )	$1e - 3$
Baseline Learning Rate ( $\alpha_b$ )	$1e - 3$
Higher Level State Model Learning Rate ( $\alpha_{hl}$ )	$5e - 4$
Regularization Coefficient ( $\lambda_{L2}$ )	$5e - 3$
Discount Factor ( $\gamma$ )	0.99
Hypernetwork Layers ( $H_a$ )	[16, 128, 128, *]
Policy Network Layers ( $f_a$ )	[64, 64, 4]
Higher Level State Model Layers ( $F_s$ )	[128, 256, 256]
Activation functions used	ReLU and its variants
Optimizer	Adam

Table 3: **Model Hyperparameters used to obtain the APC Hierarchical Planning Results in the Paper.** These were the best set of configurations among various combinations of hyperparameters that were explored. The star(\*) indicates that the final layer of hypernetwork produces weights of each layer of the policy network independently.

learns an abstract world model and plans in this abstract space. With simple planning strategies like Model Predictive Control, the APC agent can solve the task with dynamically changing goals, as observed in Figure 10 (a) in the paper.

### 2.2.2 Comparison with Lower-Level Planner

The APC agent also leverages hierarchy to plan in fewer numbers of steps. To demonstrate this, we compare against a lower-level planner. To provide the lower-level planner with the best advantage possible in competing with the APC model, we assume that the lower-level planner’s state transition model is the underlying ground truth transition function  $f_s$  capturing the transition from current to next state given an action in the environment. The lower-level planner used a Euclidean distance heuristic to get a rough estimate of a given state’s distance to goal at each planning step.

Model Predictive Control (MPC) was used to plan in both the APC and lower-level planner. We used 4-step look-ahead with random action sequences in both cases. For the APC model, we used the learned transition model  $f_s$  for the lower level and  $F_s$  for the higher level.  $F_s$  was unrolled with the random action sequence  $(\mathbf{A}_t, \mathbf{A}_{t+1}, \mathbf{A}_{t+2}, \mathbf{A}_{t+3})$ .  $N$  such random trajectories were unrolled and the sequence reaching the goal was chosen. If no such sequence was found, a random sequence was chosen and the first action was performed. This process was repeated until the goal was reached and the number of such planning steps was recorded. Note that the APC planner in this experiment had no access to heuristics that would inform the location of goal and relied only on feedback regarding whether an action sequence reached the goal.

The lower-level planner followed a similar MPC strategy, but with the added advantage of having access to the true underlying transition model and heuristics to bias action selection towards the actions that improve the heuristic measure. Even with these advantages, we found that the APC model plans dramatically faster than the lower-level planner, as seen in Figure 10 (b). This suggests that the state-action hierarchy in the APC model has the potential to greatly improve sample efficiency and exploration.

### 2.3 Code Snippet for Training a 2-Level APC Agent

```

1 import tensorflow as tf
2 import tensorflow_probability as tfp
3
4 def forward_pass(environment, abstract_action):
5
6     # The hypernetwork is used to instantiate parameters of a policy, specific to the A
7     # informed by higher layers.
8     policy_parameters = generate_policy_parameters(abstract_action)
9
10    # A dynamic policy is generated and used to navigate in the environment
11    policy = lambda x: construct_policy(x, policy_parameters)
12
13    collect_rewards, collect_log_probs, collect_l2 = [], [], []
14
15    for i in range(MAX_TIMESTEPS):

```

```
15
16     # Forward pass with the policy
17     state = environment.get_current_state()
18     action_logits = policy(state)
19
20     # Sample action and compute their probabilities
21     distribution = tfp.distributions.Categorical(logits=action_logits)
22     action = distribution.sample()
23     log_probs = distribution.log_prob(action)
24     l2 = tf.reduce_sum(tf.square(action_logits))
25
26     # Take a step in the environment
27     next_state, reward, done, _ = environment.step(action)
28
29     collect_rewards.append(reward)
30     collect_log_probs.append(log_probs)
31     collect_l2.append(l2)
32
33     if done:
34         break
35
36     # Compute loss using policy gradients
37     reinforce_loss = REINFORCE(collect_rewards, collect_log_probs, collect_l2)
38
39     return reinforce_loss
```

Listing 1: Code Snippet for Training the Hypernetwork-Modulated APC Agent ( $H_a$  and  $f_a$ ).

## 2.4 Additional Results: Zero-Shot Transfer to New Environments

We also tested the APC model on navigation problems in a variety of other large compositional building environments. The same eight higher-level “macro-actions” (options) learned for the environment in Figure 8 (a) in the paper were used by the APC model to successfully compose macro-action sequences to navigate to different goals in new environments, an example of zero-shot transfer. Example results showing hierarchical planning by the APC model in these new large environments are shown in Figure 2.

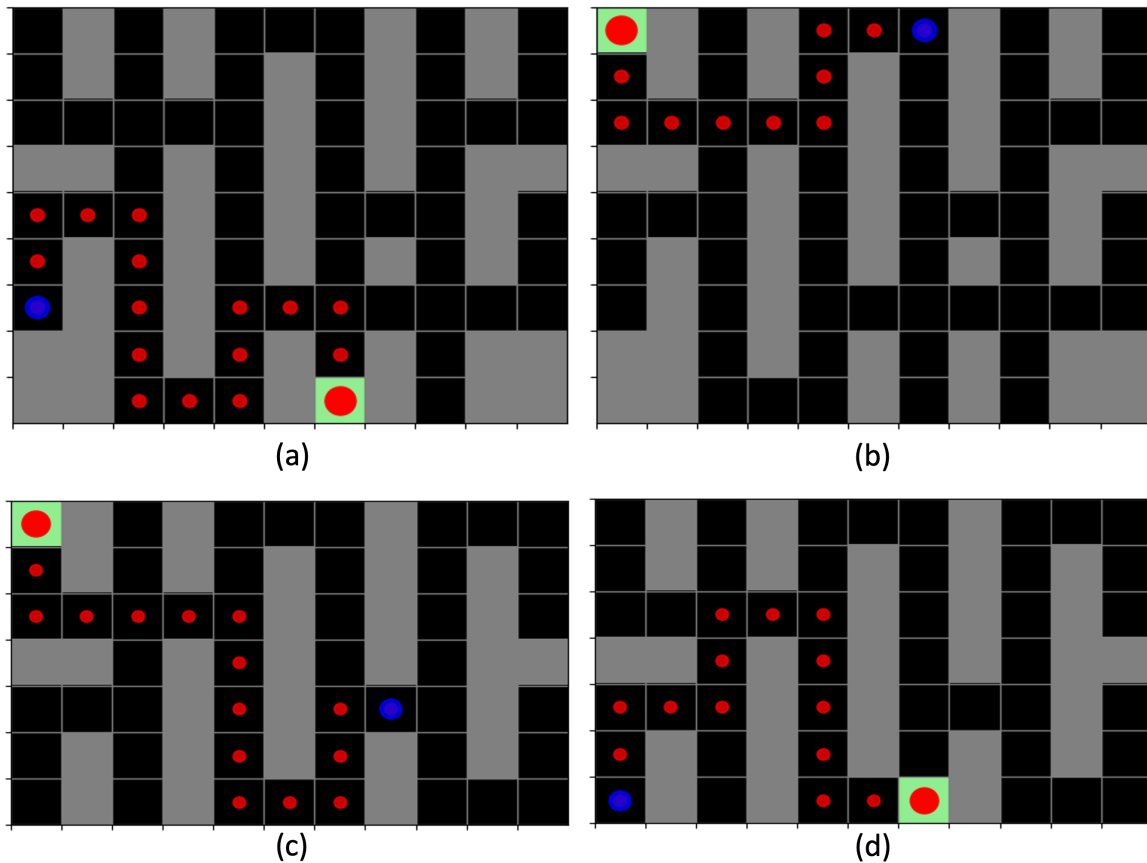


Figure 2: **Zero-Shot Transfer to New Environments.** (a)-(d) show hierarchical planning by the APC model using the same set of higher-level actions as in the paper to solve new navigation problems in new environments. Each row is a different new environment. Blue dot denotes a start state. Navigation (red dots) to two randomly chosen goals (green) are shown for each new environment.

## References

- Bacon, P.-L., Harb, J., and Precup, D. (2016). The option-critic architecture. *CoRR*, abs/1609.05140.
- Botvinick, M. M., Niv, Y., and Barto, A. G. (2009). Hierarchically organized behavior and its neural foundations: a reinforcement learning perspective. *Cognition*, 113(3):262–280.
- Chang, O., Flokas, L., and Lipson, H. (2020). Principled weight initialization for hypernetworks. In *International Conference on Learning Representations*.
- Eslami, S. M. A., Heess, N., Weber, T., Tassa, Y., Szepesvari, D., kavukcuoglu, k., and Hinton, G. E. (2016). Attend, infer, repeat: Fast scene understanding with generative models. In Lee, D., Sugiyama, M., Luxburg, U., Guyon, I., and Garnett, R., editors, *Advances in Neural Information Processing Systems*, volume 29. Curran Associates, Inc.
- Friston, K. and Kiebel, S. (2009). Predictive coding under the free-energy principle. *Philosophical transactions of the Royal Society of London. Series B, Biological sciences*, 364:1211–21.
- Galanti, T. and Wolf, L. (2020). On the modularity of hypernetworks. In *Advances in Neural Information Processing Systems*, volume 33, pages 10409–10419. Curran Associates, Inc.
- Ha, D., Dai, A. M., and Le, Q. V. (2017). Hypernetworks. In *5th International Conference on Learning Representations, ICLR 2017, Toulon, France, April 24-26, 2017, Conference Track Proceedings*. OpenReview.net.
- Hafner, D., Lillicrap, T., Norouzi, M., and Ba, J. (2021). Mastering atari with discrete world models. *9th International Conference on Learning Representations (ICLR)*.
- Hawkins, J. (2021). *A Thousand Brains: A New Theory of Intelligence*. Basic Books.
- Hinton, G. E. (2021). How to represent part-whole hierarchies in a neural network. *CoRR*, abs/2102.12627.

- Hinton, G. E., Sabour, S., and Frosst, N. (2018). Matrix capsules with EM routing. In *6th International Conference on Learning Representations, ICLR 2018, Vancouver, BC, Canada, April 30 - May 3, 2018, Conference Track Proceedings*. OpenReview.net.
- Hutsebaut-Buysse, M., Mets, K., and Latré, S. (2022). Hierarchical reinforcement learning: A survey and open research challenges. *Mach. Learn. Knowl. Extr.*, 100:172–221.
- Jiang, L., Gklezakos, D. C., and Rao, R. P. N. (2021). Dynamic predictive coding with hypernetworks. *bioRxiv*.
- Jiang, L. and Rao, R. P. N. (2022). Predictive coding theories of cortical function. *Oxford Research Encyclopedia of Neuroscience*.
- Kaelbling, L. P., Littman, M. L., and Cassandra, A. R. (1998). Planning and acting in partially observable stochastic domains. *Artif. Intell.*, 101(1-2):99–134.
- Keller, G. B. and Mrsic-Flogel, T. D. (2018). Predictive processing: A canonical cortical computation. *Neuron*, 100(2):424–435.
- Kingma, D. P. and Ba, J. (2015). Adam: A method for stochastic optimization. In *ICLR (Poster)*.
- Kosiorok, A., Sabour, S., Teh, Y. W., and Hinton, G. E. (2019). Stacked capsule autoencoders. In Wallach, H., Larochelle, H., Beygelzimer, A., d'Alché-Buc, F., Fox, E., and Garnett, R., editors, *Advances in Neural Information Processing Systems*, volume 32. Curran Associates, Inc.
- Krizhevsky, A., Sutskever, I., and Hinton, G. E. (2012). Imagenet classification with deep convolutional neural networks. In Pereira, F., Burges, C. J. C., Bottou, L., and Weinberger, K. Q., editors, *Advances in Neural Information Processing Systems*, volume 25. Curran Associates, Inc.
- Lake, B. M., Ullman, T. D., Tenenbaum, J. B., and Gershman, S. J. (2017). Building machines that learn and think like people. *Behavioral and Brain Sciences*, 40:e253.
- Lewis, M., Purdy, S., Ahmad, S., and Hawkins, J. (2019). Locations in the neocortex: A theory of sensorimotor object recognition using cortical grid cells. *Frontiers in Neural Circuits*, 13.
- Mnih, V., Heess, N., Graves, A., and kavukcuoglu, k. (2014). Recurrent models of visual attention. In Ghahramani, Z., Welling, M., Cortes, C., Lawrence, N., and Weinberger, K. Q., editors, *Advances in Neural Information Processing Systems*, volume 27. Curran Associates, Inc.
- Mountcastle, V. (1978). An organizing principle for cerebral function: the unit model and the distributed system. In Edelman, G. and Mountcastle, V., editors, *The Mindful Brain*, page 7–50. Cambridge, MA: MIT Press.
- Rao, R. P. (2010). Decision making under uncertainty: a neural model based on partially observable markov decision processes. *Frontiers in computational neuroscience*, 4:146.
- Rao, R. P. N. and Ballard, D. H. (1999). Predictive coding in the visual cortex: a functional interpretation of some extra-classical receptive-field effects. *Nature Neuroscience*, 2:79–87.
- Richards, A. (2004). *Robust constrained model predictive control*. PhD thesis, MIT.
- Sabour, S., Frosst, N., and Hinton, G. E. (2017). Dynamic routing between capsules. cite arxiv:1710.09829.
- Schneider, D. M., Sundararajan, J., and Mooney, R. (2018). A cortical filter that learns to suppress the acoustic consequences of movement. *Nature*, 561(7723):391–395.
- Sherman, S. M. and Guillery, R. W. (2013). *Functional Connections of Cortical Areas: A New View from the Thalamus*. MIT Press.
- Sutton, R. S., McAllester, D., Singh, S., and Mansour, Y. (2000). Policy gradient methods for reinforcement learning with function approximation. In Solla, S., Leen, T., and Müller, K., editors, *Advances in Neural Information Processing Systems*, volume 12. MIT Press.
- Sutton, R. S., Precup, D., and Singh, S. (1999). Between mdps and semi-mdps: A framework for temporal abstraction in reinforcement learning. *Artificial Intelligence*, 112(1):181–211.
- Wedel, M., Pieters, R., and van der Lans, R. (2022). Modeling eye movements during decision making: A review. *Psychometrika*.
- Williams, R. J. (1992). Simple statistical gradient-following algorithms for connectionist reinforcement learning. *Machine Learning*, 8:229–256.